Analytical Chemistry Insights

ORIGINAL RESEARCH

Biochemical Characteristics of Organic Matter in a Guano Concretion of Late Miocene or Pliocene Age from Manchester Parish in Jamaica

Adrian Spence[1], Richard E. Hanson[1], Toni Johnson[2], Claion Robinson[1] and Richard N. Annells[1]

[1]International Centre for Environmental and Nuclear Sciences, University of the West Indies, Mona, Kingston 7, Jamaica.
[2]Department of Chemistry, University of the West Indies, Mona, Kingston 7, Jamaica.
Corresponding author email: adrian.spence02@uwimona.edu.jm

Abstract: The biogeochemical fate of organic matter (OM) entering soils is an important issue that must be examined to better understand its roles in nitrogen cycling and as a natural modulator of soil-atmospheric carbon fluxes. Despite these critical roles, there are uncertainties in estimating the contribution of this feedback mechanism due in part to a lack of molecular-level information regarding the origin and labile and refractory inventories of OM in soils. In this study, we used a multi-analytical approach to determine molecular-level information for the occurrence and stabilization of OM in a bird guano concretion of the Late Miocene or Pliocene age in Jamaica. We determined the specific organic structures persisting in the concretion and the possible contribution of fossil organic matter to the OM pool in modern environments. Our results indicate that aliphatic species, presumably of a highly polymethylenic nature [$(CH_2)_n$], may significantly contribute to the stable soil-C pool. Although not as significant, proteins and carbohydrates were also enriched in the sample, further suggesting that fossil organic matter may contribute to carbon and nitrogen pools in present day soil organic matter.

Keywords: bird guano concretion, fossil organic matter, molecular-level, organic matter, soil organic matter, stabilization

Analytical Chemistry Insights 2013:8 41–52

doi: 10.4137/ACI.S10380

This article is available from http://www.la-press.com.

Introduction

Soil organic matter (SOM) is a complex heterogeneous mixture of various biomolecules predominantly of plant and microbial origin.[1,2] Traditionally, studies on SOM have focused on its role in soil fertility and other related soil characteristics; however, in recent decades, the role of SOM as a natural modulator of soil-atmospheric carbon fluxes has emerged as a critical area of research. Despite this shift in the conventional paradigm, knowledge of the biochemical composition and dynamics of SOM, including the carbon and nitrogen biogeochemical cycles, is based on the prerequisite that organic matter (OM) occurring in soils originates exclusively from current biomass. Conversely, the contribution and biochemical fate of fossil organic matter (FOM) to the modern SOM inventory is less well-documented and is poorly understood.[3–6] Therefore, to provide more accurate estimates of the soil-atmospheric carbon flux as well as the size and availability of the labile nitrogen pool to plants for predicting fertilizer requirements, it is important to first examine the biochemical contribution of FOM to the SOM inventory. FOM entering soil, sediment, and river environments is often released by the weathering and erosion of sedimentary and metamorphic rocks.[3,7,8]

Given the uncertainties regarding the elusive "missing carbon sinks", the size of labile and refractory SOM pools, and the dynamics of carbon and nitrogen in these pools, it is important to delineate the possible contribution of FOM to the SOM pool. Further, it has been suggested that increases in CO_2 levels are expected to continue in the next decades, even if stringent cuts in fossil fuel emissions are implemented worldwide.[8] Therefore, accurate molecular-level information about the origin of FOM, its role in the biogeochemical cycling of carbon, and processes involved in its release and transformation is necessary to provide better estimates of soil-atmospheric CO_2 fluxes. It is important to note that in addition to inputs, the composition and dynamics of biomolecules in soils are influenced by a wide range of biotic and abiotic factors. These include bioturbation, oxidation, microbial- and photo-degradation, hydrolysis, and weathering.[9]

Many of the biomolecules present in OM are reactive and are subjected to readily discernible modifications to their original molecular structure as a consequence of degradation reactions, thus allowing biogeochemical reaction sequences to be examined.[10,11] As an example, lipids demonstrate a strong preservation potential, structural specificity, and readily discernable structural modifications in OM,[11,12] and may be used to trace the origin, chemical history, and biogeochemical dynamics of OM in soils. Similarly, Copard et al[3] used fossilized geochemical markers to confirm the contribution of fossilized organic carbon (FOC) in present-day soil and river environments. Together, this information may be used to provide clues about the processes underpinning carbon and nitrogen cycling.

When considering the structural aspects of OM, it is important to examine the contribution of the various compound classes. Here we employ Fourier transform infrared (FT-IR) spectroscopy, high-resolution-magic angle spinning nuclear magnetic resonance (HR-MAS) spectroscopy, and gas chromatography mass spectrometry (GC-MS) to provide molecular-level information on the occurrence and stabilization of OM in a bird guano concretion of the Late Miocene or Pliocene age from the Manchester Parish in Jamaica. Particularly, we examined which specific organic structures persisted in the concretion and the possible contribution of FOM to the present-day OM pool. FT-IR spectroscopy has been successfully employed to study environmental matrices such as SOM[16] and compost,[17] and provides us with a non-destructive means to perform rapid molecular-level investigations of a sample. NMR spectroscopy is the single most powerful analytical technique that can be applied for the analysis of organic structures and their interactions in various environmental matrices,[18] and provides useful complementary and confirmatory data regarding specific biochemical components that persist and are available for release into the environment. Although advanced spectroscopic approaches such as HR-MAS NMR are used to yield vital data about predominant species,[18–20] these methods provide less information about exact molecular composition.[2] Therefore, we also examined the chemical decomposition of OM to yield smaller units amenable to GC-MS, thus providing a means for performing more informative investigations about the biochemical nature of the OM pool in the sample.

Methods

Sample and sample preparation

A guano concretion, previously described in Garrett et al,[21] was obtained from a goethite-rich bauxitic soil in Spitzbergen (18.1268°N, 77.4957 W and altitude 732 m) in the Manchester Parish, Jamaica. Upon receipt, the sample was thoroughly cleaned by consecutive washes with large amounts of distilled and deionized water and then oven-dried at 60 °C. Next, the concretion was subdivided, ground to a fine consistency, and sieved through a stainless steel sieve with a 2-mm aperture. Duplicate samples (15 g each) of the sieved homogenized guano concretion were exhaustively extracted with 0.1 M NaOH (each time using 30 mL), the extract filtered through 0.22-μm Durapore membrane filters (Millipore, Billerica, MA, USA) under nitrogen atmosphere, cation-exchanged [Amberlite (Rohm and Haas, Philadelphia, USA) IRC-50 (H)] to remove the Na^+ and then freeze-dried.

FT-IR analysis

The FT-IR spectrum of the sample was recorded on a PerkinElmer FT-IR Spectrum GX Spectrometer (Waltham, MA, USA). Approximately 1.0 mg of freeze-dried OM extracted from the sample was homogenized in 100 mg of spectroscopic-grade KBr with a refractive index of 1.559 and a particle size of 5–20 μm (Sigma, St. Louis, MO, USA) and used to create a disc-like potassium bromide (KBr) pellet for analysis. Background KBr spectra were obtained and spectra were compared to the background. Spectra were recorded by accumulating 256 scans (to increase the signal-to-noise ratio) in the 4000 to 400 cm^{-1} mid-infrared spectral range in the absorbance mode with a resolution of 4 cm^{-1}. Baseline correction was conducted using the automatic baseline correction method. Samples were analyzed immediately after preparation to minimize water absorption onto the hydroscopic KBr that may have obscured key signals from the sample or lead to misinterpretation of signals.[22]

High-resolution magic angle spinning (HR-MAS) NMR

Thoroughly dried organic extract (~15 mg) was placed in a 4 mm zirconium oxide rotor and 1 mL D_2O was added and titrated to pH 13.1 using NaOD (40% by wt) to ensure complete solubility. It is essential to dry the samples thoroughly and use only ampules of NaOD or D_2O to prevent a large water peak often centered at ~3.3 ppm that can obscure many actual OM signals. After homogenization of the sample using a stainless steel mixing rod, the rotor was doubly sealed using a Kel-F (Bruker) sealing ring and a Kel-F rotor cap. ^1H HR-MS NMR spectra were acquired using a Bruker 500 MHz Avance spectrometer (Billerica, MA, USA) fitted with a 4-mm triply tuned ^1H-^{13}C-^{15}N HR-MS probe fitted with an actively shielded Z gradient at a spinning speed of 10 kHz. ^1H NMR was acquired while simultaneously decoupling both ^{13}C ^{15}N nuclei. Scans (256) were acquired with a 2-s delay between pulses, a sweep width of 20 ppm, and 8 K time domain points. Basic spectral assignments were verified by two-dimensional (2D) experiments such as heteronuclear single quantum coherence (HSQC) and ^1H–^1H total correlation spectroscopy (TOCSY) of actual biopolymers (data not shown). Spectral predictions were also carried out using Advanced Chemistry Development's ACD/SpecManager and ACD/2D NMR Predictor using Neural Network Prediction algorithms (version 10.02). Parameters used for prediction including line shape, spectral resolution, sweep width, and spectrometer frequency were set to match those of the real datasets as closely as possible.[18]

Sequential solvent extraction

Solvent extraction

Total solvent extraction of the concretion followed the protocol described by Otto et al[23] with some modifications. Powdered sample (15 g) was sonicated twice for 15 min, each time with 30 mL double-distilled water to remove highly polar water-soluble compounds. Water extracts were centrifuged at 1048 xg for 30 min, decanted, and the combined extracts freeze-dried and stored at –20 °C for further analyses. The water extracted residue was freeze-dried to remove excess water and then extracted with solvents as follows: samples were sonicated twice for 15 min with 30 mL methanol, then 30 mL dichloromethane:methanol (1:1; v/v), followed by 30 mL dichloromethane. The combined total solvent extracts (''free lipids'') were filtered through glass fiber filters (Whatman GF/A, Kent, UK) using

a Buchner apparatus, concentrated by rotary evaporation, and dried completely in 2 mL glass vials under a constant stream of nitrogen gas. Solvent-extracted residues were air-dried in preparation for base hydrolysis.

Base hydrolysis

Air-dried solvent-extracted residues were refluxed for 3 h using 30 mL of 1 N methanolic KOH. The samples were allowed to cool, centrifuged for 30 min at 1048 xg, and the supernatant decanted into a glass round-bottom flask and kept at 4 °C. Each residue was then extracted twice by sonication for 15 min with 30 mL of dichloromethane:methanol (1:1; v/v). The suspensions were centrifuged as described above and the combined supernatants were acidified to pH 1 using 6 M HCl. The extracts were dried by rotary evaporation at 40 °C under vacuum and the dried extracts resuspended in 30 mL of Milli-Q water. Base hydrolyzed products were recovered from the water phase by liquid-liquid extraction in a separation funnel with diethyl ether. Anhydrous Na_2SO_4 was added to the combined ether phases to remove water. The extracts were concentrated by rotary evaporation, transferred to 2-mL glass vials, and dried under a nitrogen atmosphere. The base hydrolyzed residues were air-dried and stored at –20 °C.[24]

Derivatization and GC-MS analysis

Derivatization of total solvent extracts was performed as described below. Dried solvent extracts were redissolved in 500 µL of dichloromethane:methanol (1:1; v/v) and aliquots of the reconstituted extracts (50 µL) were evaporated to dryness under nitrogen atmosphere. The dried residues were then converted to trimethylsilyl (TMS) derivatives in a 50 µL reaction using *N*,*O*-*bis*-(trimethylsilyl)trifluoroacetamide (BSTFA) and pyridine (9:1); the reaction incubated for 2 h at 70 °C. After cooling, 50 µL of hexane was added to dilute the extracts. Gas chromatography-mass spectrometry (GC-MS) analysis of the derivatized extracts was carried out an Agilent model 6890 N gas chromatograph equipped with an Agilent 5975C InertXL mass selective detector with Triple-Axis Detector (Agilent Technologies, Santa Clara, CA, USA). Individual components were separated on a HP-5MS chemically bonded fused-silica capillary column (Hewlett-Packard, Palo Alto, CA, USA). The stationary phase consisted of 5% phenyl-95% methylpolysiloxane, and the column dimensions were as follows; 0.25 mm i.d., 0.25 µm film thickness, and 30 m length. The GC operating profile consisted of an initial temperature of 65 °C for 2 min, which was ramped at 6 °C min^{-1} up to 300 °C and held for 20 min. Separation was achieved using high purity helium (99.9995%) as the carrier gas at a flow rate of 1.0 mL min^{-1}. Approximately 1 µL of sample was autoinjected (Agilent 7683B autosampler) into the front inlet port of the GC with a 1:2 split ratio. The temperature of the port was maintained at 280 °C. The mass spectrometer was operated in standard electron impact mode (EI) at a scan range of *m*/*z* 50–650, the ion source and interface temperatures were set at 230 °C and 280 °C, respectively. Data acquisition and processing was carried out using the Agilent Chemstation G1701DA software package. Individual compounds were then identified using the NIST and Wiley MS data libraries incorporated with TMS derivatives.[23]

Results and Discussion

FT-IR spectroscopy

Extractable OM represents a complex heterogeneous mixture of biomolecules. Therefore, unlike pure compounds with characteristic sharp absorption peaks, OM extracted from the guano concretion is characterized by a series of broad bands resulting from the overlap of the absorptions of many similar functional groups (Fig. 1). In the present study, spectral

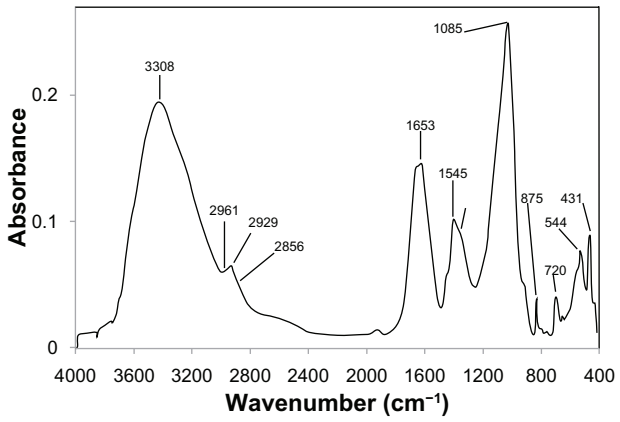

Figure 1. FT-IR spectrum of fossil organic matter extracted from a bird guano concretion of Late Miocene or Pliocene age. Major spectral assignments are consistent with data from published literature and represent the predominant species (not all species) in a given region and are assigned in the text.

assignments were consistent with those reported in the literature and represent the predominant species (not all species) in a given region, which are outlined below.

A strong broad band positioned at 3427–3308 cm^{-1} is attributed to the presence of an abundance of ν(O–H) of alcoholic or phenolic groups and ν(N–H) of amide A in the sample.[25] A band of weak to moderate absorption observed in the aliphatic C–H_x stretching region 3000–2700 cm^{-1} (most likely from lipids) comprises ν_{as}C–H of methyl groups (2961 cm^{-1}), ν_{as}C–H (2929 cm^{-1}), and νC–H (2856 cm^{-1}) from methylene groups.[26] A strong overlapping peak (1740–1600 cm^{-1} region) with a peak maximum near 1653 cm^{-1} can be assigned to aldehydes, ν(O–C=O) of esters and carboxylic acid or ν(C=O) of ketones, ν(C=C) in aromatics, ν(O–C=O) of metal-coordinate carboxylates, H-bonded ν(C=O)[27,28] and/or ν(C=O) of amides, amide I band of proteins or peptides.[25,29] The infrared spectrum also revealed a strong overlapping band at 1545 cm^{-1} attributed to the N-H in-plane bending vibration of amide II in proteins.[28] A weak shoulder near 1460 cm^{-1} is assigned to C-H bending of CH_2 and $C(CH_3)_2$ bending vibration of lipid and/or protein.[25,29] Taken together, the methylene stretching and bending bands (2929–2856 and 1460 cm^{-1}, respectively) and a weak methylene rocking band (720 cm^{-1}) indicate a long-chain linear aliphatic structure.[26,28,30] The fingerprint region from 1200–1000 cm^{-1} with a peak maximum at 1085 cm^{-1} is assigned to sugars, as well as signals (or overlaps with signals) resulting from other motions such as P=O symmetric stretching vibration of DNA.[29] Note that bands downfield of 1000 cm^{-1} are primarily of an aromatic nature.

HR-MAS NMR spectroscopy

FT-IR spectroscopy provides a good overview of the major biochemical components present in the sample (Fig. 1). However, due to the vast spectral overlap from the heterogeneity of compounds in natural organic matter, we have applied HR-MAS NMR to clarify and confirm the assignments made from the IR spectrum. The HR-MAS NMR spectrum of guano concretion-derived OM is presented in Figure 2 and provides substantial complementary details of the major biochemical components that have been preserved in the sample. Spectral regions in Figure 2 have been assigned.[20,31] The regions highlighted in brackets represent the predominant species (similar contributions from other species are present in some areas) and are broadly defined as contributions from: (1) amide signals in peptides and signals from aromatic rings including aromatic amino acid residues, some amide signals in peptides may also resonate in this area; (2) overlap region of anomeric protons from carbohydrates, protons associated with esters, protons on α carbon in peptides and double bonds; (3) other protons in carbohydrates, protons α to an ester, ether, and hydroxyl in aliphatic chains will also resonate in this region; (4) signals from various substituted methylenes and methines β to a functionality in hydrocarbons, signals from some amino acid side chains will also resonate here; (5) CH_2, main chain methylene in lipids; and (6) CH_3 groups. When a spectrum has a very strong protein contribution, the CH_3 signal is derived mainly from methyl rich amino acids residues such as leucine, isoleucine, and valine; however, when the sample is dominated by aliphatic

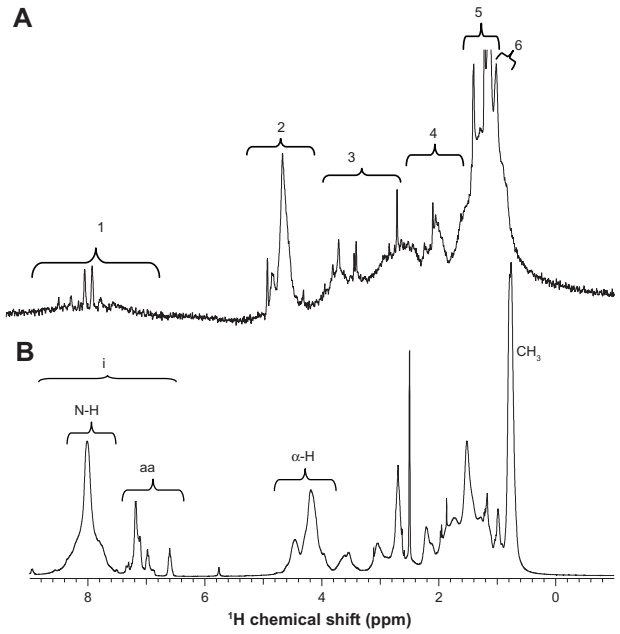

Figure 2. 1-D ^{1}H HR-MAS spectra of (**A**) fossil organic matter extracted from a bird guano concretion of Late Miocene or Pliocene age, with that of bovine serum albumin presented for comparison (**B**). General regions are highlighted in brackets and may be broadly defined as: (1) amide signals in peptides and signals from aromatic rings including aromatic amino acid residues, some amide signals in peptides may also resonate in this area; (2) overlap region of anomeric protons from carbohydrates, protons associated with esters, protons on α carbon in peptides and double bonds; (3) other protons in carbohydrates, protons α to an ester, ether, and hydroxyl in aliphatic chains will also resonate in this region; (4) signals from various substituted methylenes and methines β to a functionality in hydrocarbons, signals from some amino acid side chains will also resonate here; (5) CH_2, main chain methylene in lipids; (6) CH_3 groups; aa = amino acids; and (i) mainly aromatic residues.

chains, for example in Figure 2, a considerable contribution is from aliphatic substances.[20,31]

It is evident that the 1-D NMR spectrum is dominated by signals from aliphatic lipids (regions 5 and 6), suggesting these compounds are selectively preserved and may be a major contributor to the soil-C pool. This enrichment of aliphatic lipids in the sample may be due in part to their hydrophobic nature, which prevents transport and as a result, lowers the contact with degrading microbes and other biotic and abiotic factors, allowing them to remain in the sample for longer periods of time. Additionally, aliphatic enrichment may be due in part to the degradability of the readily bioavailable dissolved or water-extractable OM fraction. This is consistent with the observation that alkyl-C, such as those in polymethylenic structures, is the most recalcitrant form of organic carbon found in non-living SOM.[32,33] Such structures have also been found in the resistant biopolymers of algae.[34] Further, several recent studies focusing on the adsorption of OM to clay mineral surfaces have demonstrated the aliphatic nature of clay-organo interactions.[35–38] Such interactions should not be excluded from the enrichment of aliphatic species in the sample. Although not as significant as aliphatic lipids, there is some evidence to suggest that carbohydrates have been preserved in the sample. This is somewhat surprising since the conventional view is that labile substrates such as carbohydrates are rapidly mineralized by degrading microbes. It is probable that the preservation of carbohydrates in the sample is linked to modifications by other biomolecules such as lipids or proteins. For instance, recalcitrant lipopolysaccharides are thought to be a large component of the surviving carbohydrates entering the SOM pool.[2,18,31]

Similarly, the presence of proteins/peptides (region 1) in the sample is somewhat unexpected. Proteins/peptides have been confirmed by the spectral similarity shown in Figure 2B (protein standard bovine serum albumin) to that of the 1D ^{1}H NMR spectrum of the sample (Fig. 2A), for which contributions from protein/peptide structures such as amide (N-H), aromatic amino acids (aa), and α-protons are easily distinguished. Traditionally, proteins are thought to be labile in the environment; therefore, it is not immediately clear whether specific proteins presented here are resistant to degradation due to their intrinsic molecular structure, as is the case for membrane proteins,[39] or environmentally induced modifications of their quaternary structures and physico-chemical (charge and hydrophobicity/hydrophilicity) and biochemical characteristics. For example, the biorefractory nature of signals resonating from lipoproteins (region 4) has previously been demonstrated.[31] Additionally, protein preservation could include abiotic processes such as condensation reactions, which are known to reduce degradability.[42] Similarly, sorptive protection offered by mineral matrix may be an important factor in the long-term stabilization of proteins/peptides. It has been suggested that this form of association with clay minerals may result in OM being isolated in microenvironments where it could be protected from decomposers.[43] It is also intriguing to suggest that proteins/peptides survived as products of humification catalyzed clay-mediated reactions before concretion of the sample. This suggestion is favored since proteins/peptides are structurally and biochemically versatile biomolecules (they contain both cationic and anionic functional groups as well as hydrophilic and hydrophobic residues) and have demonstrated a strong affinity for clay mineral surfaces.[37,38] Additionally, anoxic soil conditions may have also contributed to the overall stability of OM in the sample as fossilization occurred. Whatever the case, these results further suggest that FOM may be an important contributor to carbon and nitrogen pools in present-day SOM.

Lipid analysis

To further understand the nature of the dominant lipid fraction in the sample, we performed GC-MS analysis of silylated lipid extracts. The major classes of compounds contained in the fractions obtained from sequential extraction of the sample included a series of *n*-alkanoic acids (*n*-C_7, *n*-C_{16}, *n*-C_{18}), α-alkanedioic acids (C_3–C_9) with a slight even-over-odd predominance, and α-hydroxyalkanoic acids (C_3–C_6) with both normal- and *iso*-branched structures. Branched-chain [*iso*-(C_4) and *anteiso*-(C_5)] fatty acids were also detected in the base-hydrolyzed sample at relatively low levels (Table 1). Other compounds detected in the sample in trace amounts included two proteinogenic amino acids (L-enantiomers), glycine and proline, the amino acid degradation product urea, the branched chain fatty alcohol 5-nonanol, a low-molecular-weight organic acid (acetic acid), and a series of

Table 1. Occurrence of identified compounds in fractions obtained from sequential extraction of a fossilized bird guano.

Compound	MW	Composition[a]	CAS number
n-Alkanoic acids			
Heptanoic acid	130	$C_7H_{14}O_2$	111-14-8
Hexadecanoic acid	256	$C_{16}H_{32}O_2$	57-10-3
Octadecanoic acid	284	$C_{18}H_{36}O_2$	57-11-4
n-Alkanedioic acids			
Propanedioic acid	104	$C_3H_4O_4$	141-82-2
Butanedioic acid	118	$C_4H_6O_4$	110-15-6
2-Methylbutanedioic acid	132	$C_5H_8O_4$	498-21-5
3-Methylpentanedioic acid	146	$C_6H_{10}O_4$	626-51-7
Hexanedioic acid	146	$C_6H_{10}O_4$	124-04-9
Octanedioic acid	174	$C_8H_{14}O_4$	505-48-6
Nonanedioic acid	188	$C_9H_{16}O_4$	123-99-9
Hydroxyalkanoic acids			
α-Hydroxypropanoic acid	90	$C_3H_6O_3$	50-21-5
2-Methy-2-hydroxypropanic acid	104	$C_4H_8O_3$	594-61-6
3-Methylpentanoic acid	116	$C_6H_{12}O_2$	105-43-1
4-Methylpentanoic acid	116	$C_6H_{12}O_2$	646-07-1
4-Methyl-2hydroxypentaanoic acid	132	$C_6H_{12}O_3$	13748-90-8
α-Hydroxyhexanoic acid	132	$C_6H_{12}O_3$	6064-43-7
Other compounds			
Urea	60	CH_4N_2O	57-13-6
Acetic acid	60	CH_4N_2O	64-19-7
Glycine	75	$C_2H_5NO_2$	56-40-6
Proline	115	$C_5H_9NO_2$	147-85-3
Benzamide	121	C_7H_7NO	55-21-0
Benzoic acid	122	$C_7H_6O_2$	65-85-0
4-Hydroxybenzoic acid	138	$C_7H_6O_3$	99-96-7
5-Nonanol	144	$C_9H_{20}O$	623-93-8
Benzenepropanoic acid	150	$C_9H_{10}O_2$	501-52-0

Note: [a]Compounds are presented without the TMS group for simplicity and ease of interpretation.

normal and substituted benzoic acid (phenylalkanoic acids). The dominant compound in the extracts was C_3 alkanedioic acid (Fig. 3), while α-alkanedioic acids represent the dominant class of compounds in the sample.

It has been hypothesized that, in the environment, the reactivity and therefore lability of aliphatic chains increases with their degree of unsaturation; hence, it is not surprising that we did not detect *n*-alkenoic acids in the combined lipid extracts. Hydroxylation of unsaturated carbon centers may have resulted in the disappearance of *n*-alkenoic acids and a concomitant increase in the number of hydroxyl FAs in the sample. If this hypothesis is correct, it would account in part for the hydroxyl FAs detected in the sample (Table 1). Additionally, unsaturated FAs may have been oxidized to their respective epoxy acids (epoxidation). However, epoxides have been found to be very labile,[45] which may therefore explain why they were not detected in the sample. Epoxides may further undergo hydrolysis to yield mono- and/or di-hydroxyacids; however, we did not detect di-hydroxyacids in the sample. Similarly, the lack of compounds of the class *n-alkanes* in the sample was not unexpected since compounds of this class are typically among the first to degrade. The dominance of compounds ≤12 C long in the sample was somewhat surprising as it has been demonstrated that the degradation rate constant of short-chain FAs is twice that of their longer-chain counterparts.[47]

Although not present in significant diversity or relative abundance, there is still sufficient evidence to support the recalcitrance of guano-derived lipids in this study. This recalcitrance may be due in part to the molecular structure, cross linkages, and various mechanisms of protection offered by minerals. The roles of specific mineral components (Fe, Al, and Si) in clay-organo interactions have been

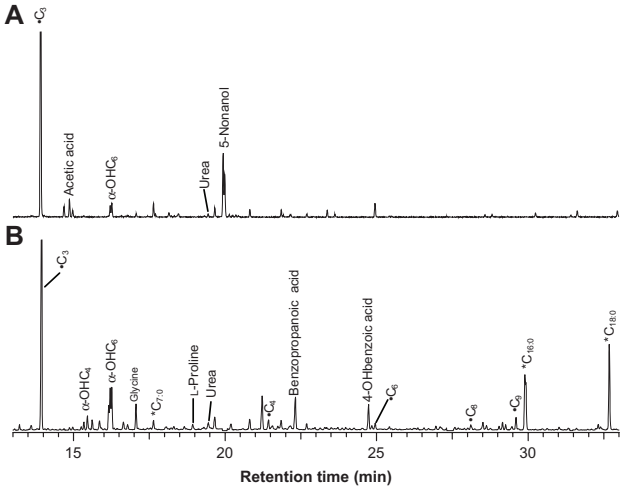

Figure 3. Representative GC-MS chromatograms (TIC) of fractions obtained from sequential solvent extraction of a bird guano concretion of Late Miocene or Pliocene age. (**A**) Free lipids and (**B**) bound lipids (base hydrolysate). * denotes *n*-alkanoic acids and • denotes *n*-alkanedioic acids.

previously suggested.[38] Further, selective preservation of shorter chain FAs after degradation may be linked to chemical modification by polar cellular components, such as amino acids and carbohydrates, as is consistent with lipoproteins and lipopolysaccharides, respectively. Such biomolecules have been shown to resist decomposition in soil microbial biomass and leachates.[31] The biorefractory nature of *n*-C_{16}, *n*-C_{18} in dissolved organic matter (DOM) and soil has been previously demonstrated[48] and may explain the relative abundance of these compounds detected in the sample. Further, hexadecanoic acid (*n*-C_{16}) may have accumulated since it is a key intermediate of oleic acid (*n*-C_{18}) degradation.

Conclusion

The biochemical contribution of FOM to the SOM inventory is important and must be considered in order to provide more accurate estimates of the soil-atmospheric carbon flux as well as size and availability of the labile nitrogen pool to plants so as to predict fertilizer requirements aimed at improving nitrogen use efficacy. Molecular-level investigations were carried out to determine the possible contribution of FOM to the OM pool in soils. The results indicate the occurrence of major biochemical components (proteins, carbohydrates, and various classes of lipids) in a guano concretion. Although not a quantitative approach, this study provides a useful molecular-level descriptor of FOM components preserved in a concretion synonymous with that of sedimentary rocks. Therefore, it is probable that fossil components preserved in the concretion are available for release by weathering and erosion, eventually becoming integrated into the recent SOM pool. These findings also further highlight uncertainties in our knowledge of SOM inventory and its role in regulating natural and anthropogenic changes to global carbon and nitrogen biogeochemical cycles. Therefore, if we are to realistically address these and related concerns, further studies are needed to decipher the fate of FOM in the environment and establish a link between FOM in soils, sediments, and rivers as well as the carbon and nitrogen biogeochemical cycles.

Acknowledgements

We are grateful to Charles Grant and Johann Antoine of the International Centre for Environmental and Nuclear Sciences (ICENS) and Dr. Sherene James-Williamson of the department of Geography and Geology, University of the West Indies, Mona for their efforts in acquiring the guano concretion. We thank the anonymous reviewers for their insights and help with the completion of this manuscript.

Author Contributions

Conceived and designed the experiments: AS. Analyzed the data: AS, REH, TJ, CR. Wrote the first draft of the manuscript: AS. Contributed to the writing of the manuscript: AS, REH, TJ, CR, RNA. Agree with manuscript results and conclusions: AS, REH, TJ, CR, RNA. Jointly developed the structure and arguments for the paper: AS, REH, CR. Made critical revisions and approved final version: AS, RNA. All authors reviewed and approved of the final manuscript.

Funding

Author(s) disclose no funding sources.

Competing Interests

Author(s) disclose no potential conflicts of interest.

Disclosures and Ethics

As a requirement of publication the authors have provided signed confirmation of their compliance with ethical and legal obligations including but not limited to compliance with ICMJE authorship and competing

interests guidelines, that the article is neither under consideration for publication nor published elsewhere, of their compliance with legal and ethical guidelines concerning human and animal research participants (if applicable), and that permission has been obtained for reproduction of any copyrighted material. This article was subject to blind, independent, expert peer review. The reviewers reported no competing interests.

References

1. Kögel-Knabner I. Analytical approaches for characterizing soil organic matter. *Organic Geochemistry*. 2000;31(7–8):609–25.
2. Kögel-Knabner I. The macromolecular organic composition of plant and microbial residues as inputs to soil organic matter. *Soil Biology and Biochemistry*. 2002;34(2):139–62.
3. Copard Y, Di-Giovanni C, Martaud T, Albéric P, Olivier J-E. Using Rock-Eval 6 pyrolysis for tracking fossil organic carbon in modern environments: implications for the roles of erosion and weathering. *Earth Surface Processes and Landforms*. 2006;31(2):135–53.
4. Di-Giovanni C, Disnar JR, Campy M, Macaire JJ. Variability of the ancient organic supply in modern humus. *Analusis*. 1999;27(5):398–401.
5. Di-Giovanni C, Disnar JR, Bichet V, Campy M, Guillet B. Geochemical characterization of soil organic matter and variability of past glacial detrital organic supply (Chaillexon lake, France). *Earth Surface Processes and Landforms*. 1998;23(12):1057–69.
6. Graz Y, Di-Giovanni C, Copard Y, et al. Occurrence of fossil organic matter in modern environments: optical, geochemical and isotopic evidence. *Applied Geochemistry*. 2011;26(8):1302–14.
7. Blair NE, Leithold EL, Ford ST, Peeler KE, Holmes JC, Perkey. The persistence of memory: the fate of ancient sedimentary organic carbon in a modern sedimentary system. *Geochemica et Cosmochimica Acta*. 2003; 67(1):63–73.
8. Watson RT, Rodhe H, Oeschger H, Siegenthaler U. Greenhouse gases and aerosols prepared by Working Group I. In: Haughton JT, Jenkins GJ, Ephraums JJ, editors. Climate Change: The IPCC Scientific Assessment. Cambridge, UK: Cambridge University Press; 1990:1–40.
9. Naafs DFW, van Bergen PF, de Jong MA, Oonincx A, de Leeuw JW. Total lipid extracts from characteristic soil horizons in a podzol profile. *European Journal of Soil Science*. 2004;55(4):657–69.
10. Colombini MP, Giachi G, Modugno F, Ribechini E. Characterisation of organic residues in pottery vessels of the Roman age Antinoe (Egypt). *Microchemical Journal*. 2005;79(1–2):83–90.
11. Colombini MP, Modugno F, Ribechini E. Organic mass spectrometry in archaeology: evidence for Brassicaceae seed oil in Egyptian ceramic lamps. *J Mass Spectrom*. 2005;40(7):890–8.
12. Grossi V, Caradec S, Gilbert F. Burial and reactivity of sedimentary microalgal lipids in bioturbated Mediterranean coastal sediments. *Marine Chemistry*. 2003;81:57–69.
13. Nierop KG, Verstraten JM. Rapid molecular assessment of the bioturbation extent in sandy soil horizons under pine using ester-bound lipids by on-line thermally assisted hydrolysis and methylation-gas chromatography/mass spectrometry. *Rapid Commun Mass Spectrom*. 2004;18(10):1081–8.
14. Sun M-Y, Zou L, Dai J, Ding H, Culp RA, Scranton MI. Molecular carbon isotopic fractionation of algal lipids during decomposition in natural oxic and anoxic seawaters. *Organic Geochemistry*. 2004;35(8):895–908.
15. Schulze WX. Protein analysis in dissolved organic matter: what proteins from organic debris, soil leachate and surface water can tell us—a perspective. *Biogeosciences*. 2005;2:75–86.
16. Réveillé V, Mansuy L, Jardé E, Garnier-Sillam E. Characterisation of sewage sludge-derived organic matter: lipids and humic acids. *Organic Geochemistry*. 2003;34(4):615–27.
17. Grube M, Lin JG, Lee PH, Kokorevicha S. Evaluation of sewage sludge-based compost by FT-IR spectroscopy. *Geoderma*. 2006;130(3–4): 324–33.
18. Kelleher BP, Simpson MJ, Simpson AJ. Assessing the fate and transformation of plant residues in the terrestrial environment using HR-MAS NMR Spectroscopy. *Geochimica et Cosmochimica Acta*. 2006;70(16):4080–94.
19. Simpson AJ, Song G, Smith E, Lam B, Novotny EH, Hayes MHB. Unraveling the structural components of soil humin by use of solution-state nuclear magnetic resonance spectroscopy. *Environ Sci Technol*. 2007;41(3):876–83.
20. Simpson AJ, Simpson MJ, Smith E, Kelleher BP. Microbially derived inputs to soil organic matter: are current estimates too low? *Environ Sci Technol*. 2007;41(23):8070–6.
21. Garrett RA, Porter ARD, Hunt PA. An occurrence of cadmiferous phosphorite soil concretions in Jamaica. *Applied Geochemistry*. 2010;25(7):1047–55.
22. Frost RL, Kloprogge JT, Thi Tran TH, Kristof J. The effect of pressure on the intercalation of an ordered kaolinite. *American Mineralogist*. 1998;83(11–12):1182–7.
23. Otto A, Chubashini S, Simpson MJ. A comparison of plant and microbial biomarkers in grassland soils from the Prairie Ecozone of Canada. *Organic Geochemistry*. 2005;36(3):425–48.
24. Otto A, Simpson MJ. Analysis of soil organic matter biomarkers by sequential chemical degradation and gas chromatography-mass spectrometry. *J Sep Sci*. 2007;30(2):272–82.
25. Marshall CP, Carter EA, Leuko S, Javaux E. Vibrational spectroscopy of extant fossil microbes: relevance for the astrobiological exploration of Mars. *Vibrational Spectroscopy*. 2006;41(2):182–9.
26. Marshall PC, Javaux EJ, Knoll AH, Walter MR. Combined micro-Fourier transform infrared (FTIR) spectroscopy and micro-Raman spectroscopy of Proterozoic acritarchs: a new approach to palaeobiology. *Precambrian Research*. 2005;138(2–4):208–24.
27. Mangrich AS, Lobo MA, Tanck CB, Wypych F, Toledo EBS, Guimarães E. Criterious preparation and characterization of earthworm-composts in view of animal waste recycling. Part I. Correlation between chemical, thermal and FTIR spectroscopic analyses of four humic acids from earthworm-composted animal manure. *Journal of the Brazilian Chemical Society*. 2000;11(11):164–9.
28. Smidt E, Eckhardt K-U, Lechner P, Schulten H-R, Leinweber P. Characterization of different decomposition stages of biowaste using FT-IR spectroscopy and pyrolysis-field ionization mass spectrometry. *Biodegradation*. 2005;16(1):67–79.
29. Santivarangkna C, Wenning M, Foerst P, Kulozik U. Damage of cell envelope of *Lactobacillus helveticus* during vacuum drying. *J Appl Microbiol*. 2007;102(3):748–56.
30. Wei Z, Xi B, Zhao Y, Wang S, Liu H, Jiang Y. Effects of inoculating microbes in municipal solid waste composting on characteristics of humic acid. *Chemosphere*. 2007;68(2):368–74.
31. Spence A, Simpson AJ, McNally DJ, et al. The degradation characteristics of microbial biomass in soil. *Geochimica et Cosmochimic Acta*. 2011;75(10):2571–81.
32. Baldock JA, Massiello CA, Gelinas Y, Hedges. Cycling and composition of organic matter in terrestrial and marine ecosystems. *Marine Chemistry*. 2004;92(1–4):39–64.
33. Kindler R, Miltner A, Thullner M, Richnow H-H, Kästner M. Fate of bacterial biomass derived fatty acids in soil and their contribution to soil organic matter. *Organic Geochemistry*. 2009;40(1):29–37.
34. Derenne S, Le Berre F, Largeau C, Hatcher PG, Connan J, Raynaud FF. Formation of ultralaminae in marine kerogens via selective preservation of thin resistant outer walls of microalgae. *Organic Geochemistry*. 1992;19(4–6):345–50.
35. Feng X, Simpson AJ, Simpson MJ. Chemical and mineralogical controls on humic acid sorption to clay mineral surfaces. *Organic Geochemistry*. 2005;36(11):1553–66.
36. Feng X, Simpson AJ, Simpson MJ. Investigating the role of mineral-bound humic acid in phenanthrene sorption. *Environ Sci Technol*. 2006;40(10):3260–6.
37. Simpson AJ, Simpson MJ, Kingery WL, et al. The application of 1H high-resolution magic-angle spinning NMR for the study of clay–organic associations in natural and synthetic complexes. *Langmuir*. 2006;22(10): 4498–508.

38. Spence A, Kelleher BP. FT-IR spectroscopy analysis of kaolinite-microbial interactions. *Vibrational Spectroscopy*. 2012;61:151–5.
39. Yamashita Y, Tanoue E. Chemical characteristics of amino acid-containing dissolved organic matter in seawater. *Organic Geochemistry*. 2004;35(6): 679–92.
40. Nguyen RT, Harvey HR. Preservation of protein in marine systems: hydrophobic and other noncovalent associations as major stabilizing forces. *Geochimica et Cosmochimica Acta*. 2001;65(9):1467–80.
41. Nguyen RT, Harvey HR. Preservation via macromolecular associations during Botryococcus braunii decay: proteins in the Pula Kerogen. *Organic Geochemistry*. 2003;34(10):1391–403.
42. Nagata T, Kirchman DL. Roles of submicron particles and colloids in microbial food webs and biogeochemical cycles within marine environments. In: Jones T, editor. *Advances in Microbial Ecology*. New York, NY: Plenum. 1997;81–103.
43. Salmon V, Derenne S, Lallier-Vergès E, Largeau C, Beaudoin B. Protection of organic matter by mineral matrix in a Cenomanian black shale. *Organic Geochemistry*. 2000;34(5):463–74.
44. Goni MA, Hedges JI. The diagenetic behavior of cutin acids in buried conifer needles and sediments from a coastal marine-environment. *Geochimica et Cosmochimica Acta*. 1990;54(11):3083–93.
45. Stephanou EG, Stratigakis N. Oxocarboxylic and α,β-dicarboxylic acids: photooxidation products of biogenic unsaturated fatty acids present in urban aerosols. *Environ Sci Technol*. 1993;27:1403–7.
46. Michaels BC, Ruettinger RT, Fulco AJ. Hydration of 9,10-epoxypalmitic acid by a soluble enzyme from Bacillus megaterium. *Biochem Biophys Res Commun*. 1980;92(4):1189–95.
47. Sun M-Y, Wakeham SG. Molecular evidence for degradation and preservation of organic matter in the anoxic Black Sea Basin, *Geochimica et Cosmochimica Acta*. 1994;58(16):3395–406.
48. Jandl G, Schulten H-R, Leinweber P. Quantification of long-chain fatty acids in dissolved organic matter and soils. *Journal of Plant Nutrition and Soil Science*. 2002;165(2):133–9.

Supplementary Figure

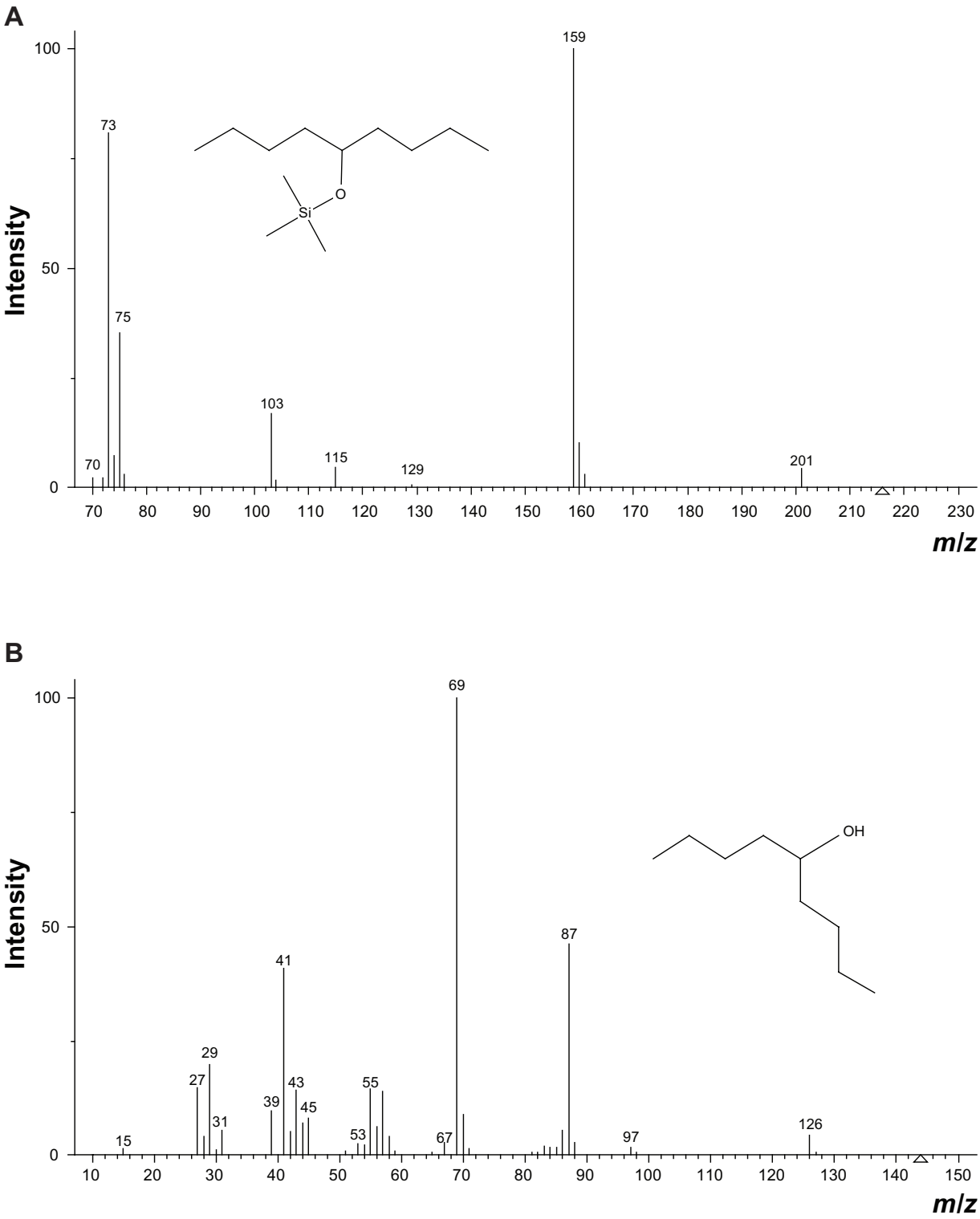

Figure S1. (*Continued*)

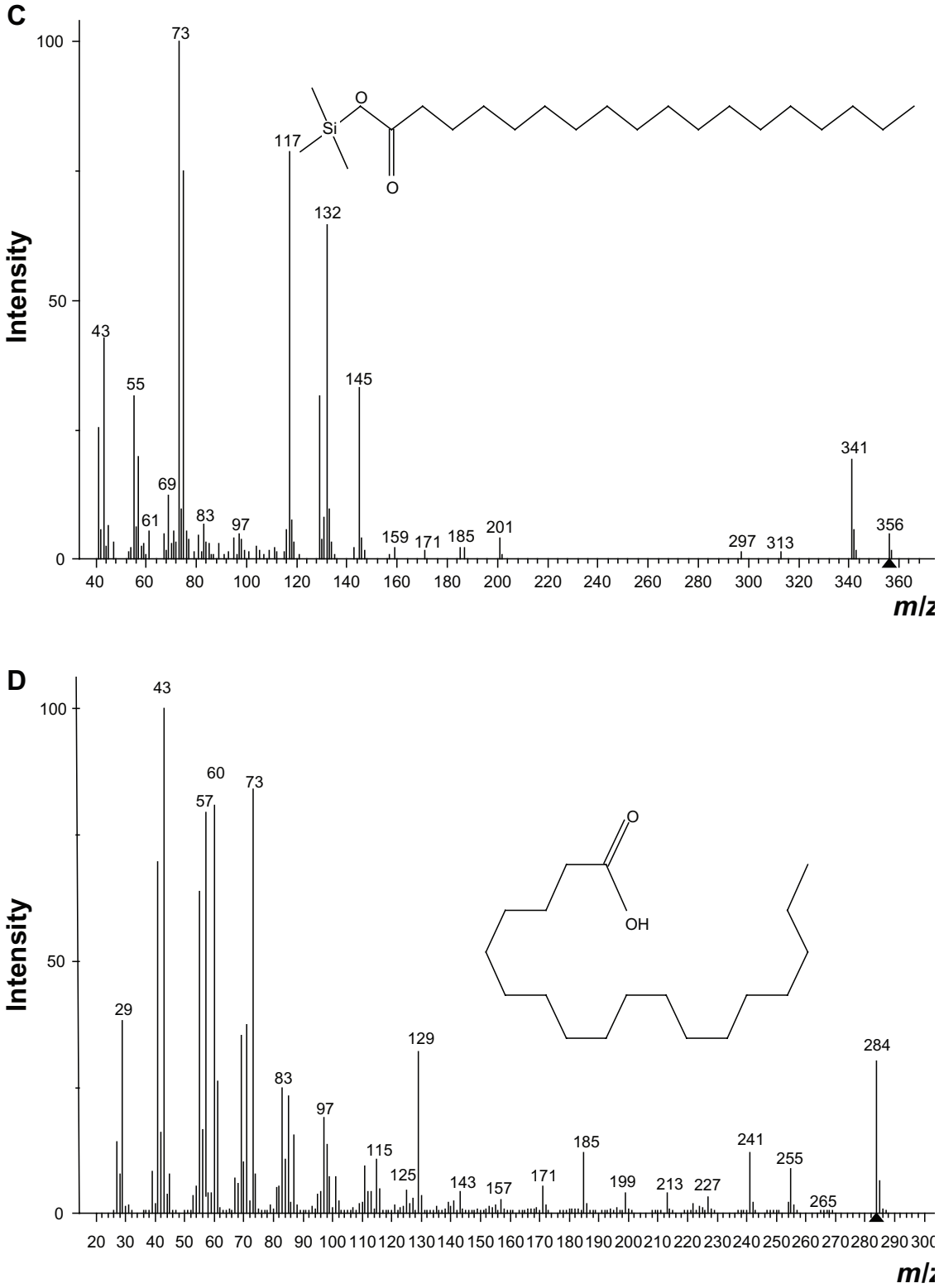

Figure S1. Mass spectra of selected compounds (with and without TMS) identified from sequential solvent extraction of a guano concretion of Late Miocene or Early Pliocene age from Manchester Parish in Jamaica. (**A**) Nonanol-5-TMS showing characteristic fragment ion peaks at *m*/*z* 73 and 159 resulting from $Si(CH_3)_3$ and $C_8H_{19}OSi$ fragment ions, respective; (**B**) 5-nonanol showing characteristic fragment ion peaks at *m*/*z* 69 and 87, and are attributed to C_5H_9 and $C_5H_{11}O$ fragment ions, respectively; (**C**) octadecanoic acid-TMS showing prominent fragment ions at *m*/*z* 73 and 132 which have been generated by $Si(CH_3)_3$ and $C_5H_{12}O_2Si$ fragment ions, respectively; and (**D**) octadecanoic acid showing characteristic ion peaks at *m*/*z* 43 (C_3H_7), 73 (C_3H_5O), and 129 ($C_7H_{13}O_2$).